European Review for Medical and Pharmacological Sciences 2018; 22: 1233-1240

Morphologic and molecular alteration during tibia fracture healing in rat

M.-D. YU, B.-H. SU, X.-X. ZHANG

Department of the Spine Surgery II, Weifang People's Hospital, Weifang, China

Abstract. – OBJECTIVE: To monitor morphological feature and related osteogenic and bone metabolic change during healing of tibia fracture in a rat model.

MATERIALS AND METHODS: Tibia density and trabecular thickness were evaluated. Histopathology was examined by HE staining. Serous inflammatory factors IL-4, IL-6, TNF-α and metabolic biomarkers ALP, β-CTX, P1NP, were determined by ELISA. The expression of RUNX2, TGF-β1, VEGF-α, BMP-2, BMP-4, and BMP-7 in callus tissue were qualified by RT-PCR.

RESULTS: Bone density decreased until week 4 and then increased post-operation. Trabeculae in callus were thickened over time with active osteogenesis. ELISA indicated the most severe inflammation at week 2, with the highest level of TNF-α, IL-6, and the lowest level of IL-4. After 4 weeks, the inflammation was alleviated accompanying with the decline of TNF-α and IL-6, while there was the elevation of IL-4. Bone metabolism showed active osteogenesis and resorption at week 6 with high P1NP and β-CTX. The expression of RUNX2, TGF-β1, VEGF-α, BMP-2, BMP-4, and BMP-7 increased progressively from week 1 to 6. The major lesions at week 2 in sham were tissue necrosis, periosteal reactive hyperplasia, inflammatory cell infiltration, capillary hyperplasia and slight fibro-blast cytopoiesis. At week 4, proliferation was greatly activated, fibrous callus shaped and chondrogenesis and some osteogenesis occurred at week 8.

CONCLUSIONS: In rat model, bone density started to increase at week 6 after fracture, accompanied with *trabeculae* thickening, serous inflammatory factors decline, and peaked bone morphogenetic protein/growth factors, which indicated active osteogenesis was conforming to the classical phase of secondary fracture healing.

Key Words:

Tibia fracture, Bone density, Trabecular thickness, Inflammatory factors, Bone metabolism, Bone morphogenetic protein.

Abbreviations

TNF = tumor necrosis factor; IL = Interleukin; CCL2 = chemokine (C-C motif) ligand 2; MSC = mesenchymal stem cells; RUNX2 = Runt-related transcription factor 2; TGF = Tumor growth factor; VEGF = Vascular endothelial growth factor; BMP = Bone morphogenetic protein; BMD = bone mineral density; ELISA = Enzyme linked immunosorbent assay; ALP = alkaline phosphatase; βCTX = β cross-linked C-telopeptide of type 1 collagen; P1NP = procollagen type 1 N-terminal propeptide; EDTA = ethylenediaminetetraacetic acid; SD = standard deviation.

Introduction

Fractures are common traumatic injuries tightly associated with senile osteoporosis, which affect 50% of women and 25% of men over age 50 worldwide[1]. Its clinical management and repair are important issues for orthopedic surgeon and specialists. Medical cares for these diseases impose heavily social and economic burden on our community[2]. The clear understanding of the fundamental biology underlying fracture is urgently needed for optimal clinical intervention and treatment.

Bone is a complex and dynamic organ composed by diversified cells[3]. The maintenance of intrinsic homeostasis of minerals metabolism and differentiation is essential for its physiological functions[4]. Mechanic damage induces acute inflammatory reaction[5], followed by resorption process mediated by osteoclast[6]. Macrophage phase transformation, recruitment of mesenchymal stem cells and osteoblast differentiation are initiated to repair the damage[7]. Inflammation is the first line of defense against fracture[8]. The mechanic disruption of vasculature results in activation of plasma coagulation and platelet[9]. Local exposed of necrotic cell, macrophage and deformed extracellular matrix release signaling factors to attract cascades of inflammatory cell[10]. In addition to its role in clearance of dead cell and bone debris, inflammatory cells also are the source of the second wave of molecular cues such as tumor necrosis factor (TNF)-α, Interleukin (IL)-1β, IL-6 and chemokine (C-C motif) ligand 2 (CCL2) in

Corresponding Author: Xiaoxia Zhang, MD; e-mail: zhangxiaoxiaxiaa@163.com

recruitment of fibroblasts, mesenchymal stem cells and osteoprogenitor cells[11]. Platelet and macrophage-derived growth factors guide proliferation, differentiation, and maturation of these cells, which eventually develop into granulation tissues and neovasculature[12]. Hypoxia in the center of fracture sites stimulates differentiation of mesenchymal stem cells (MSC) into chondrocyte, which extends to bridge the broken ends[13]. However, normoxia in periosteum induces differentiation of MSC towards osteoblast and production of woven bone[14]. Once apoptosis program initiated in chondrocyte, calcium is released to induce vascular ingrowth and calcification, which termed as callus formation[15]. At the final stage, Haversian system is restored via removal cartilage and woven bone by chondroclasts and osteoclasts[16].

Tibia is the major bone of the lower leg. Tibia fracture generally could be divided into three categories based on the location of the injury, shaft fractures, plateau fracture and plafond fracture[17]. Many factors should be taken into consideration to make the surgical treatment strategy including pin, plate, screw, rod, etc. In this study, we used a rat model of tibia fracture, carefully characterized the morphologic, pathologic and molecular progression during bone healing, demonstrating a classical secondary fracture healing.

Materials and Methods

Animal Model

SPF-grade SD rats were obtained from National Accelerator Laboratory Animal Center (Shanghai, China). All rats were housed in a pathogen-free environment. The experimental protocols were approved by the Ethical Committee of Animal Care and Use. All animal work was performed in strict accordance with the approved protocol. In total, 50 rats with average body weight 250-300 g were equally and randomly divided into two groups for control or surgery respectively. The treatment group rats were intraperitoneally anesthetized with 10% chloral hydrate first. After preoperative skin preparation and sterilization, the knee joint and middle tibia on the right side were exposed, and the open fracture was introduced by carborundum disc. Kirschner wire was inserted into the tibial incision to fix the intramedullary nail. The leg was immobilized by plaster after wound sutured. Penicillin (10^5 U/d) was administrated intramuscularly for 3 consecutive days for infection control.

RT-PCR

The primers used in this study were as follow:
Runt-related transcription factor 2 (RUNX2):
Forward: 5'-GCACAAACATGGCCAGTTCA-3'
Reverse: 5'-AAGCCATGGTGCCCGTTAG-3'
Tumor growth factor (TGF)-β1: Forward: 5'-TGGAGCAAC ATGTGGAACTC-3'
Reverse: 5'-GTCAGCAGCCGGTTACCA-3'
Vascular endothelial growth factor (VEGF)-α:
Forward: 5'-CCTGGCCCTCAAGTACACCTT-3'
Reverse: 5'-ACATCTGCTGTGCTGTAGGAAG-3'
Bone morphogenetic protein (BMP)-2: Forward: 5'-TTCTGTCCCTACTGATGAGTTTCTC-3'
Reverse: 5'-AAGTCACTAGCAGTGGTCTTACCTG-3'
BMP-4: Forward: 5'-AGCATGTCAGGATTAGCCGA-3'
Reverse: 5'-TGGAGATGGCACTCAGTTCA-3'
BMP-7: Forward: 5'-TCCGGTTTGATCTTTCCAAGA-3'
Reverse: 5'-CCCGGATGTAGTCCTTATAGATCCT-3'
β-actin: Forward: 5'-ACTATTGGCAACGAGCGGTT-3'
Reverse: 5'-CAGGATTCCATACCCAAGA AGGA-3'

The total RNA was extracted with TRIzol reagent and quality checked for purity and integrity. The first strand cDNA was synthesized with PrimeScript RT reagent kit (TaKaRa Bio, Dalian, Liaoning, China). The RT-PCR was conducted with SYBR Green Master kit (Promega, Madison, WI, USA) in according to the manufacturer's instruction. The PCR conditions were as following: 98°C denature for 30 s, 60°C annealing for 30 s, 68°C extension for 30 s by 35 cycles, followed by 68°C extra extension for 5 min. The bands were visualized with EB staining and analyzed with ImageJ software. The relative expression was calculated and normalized to β-actin. The results are representative of at least three independent experiments.

Measurement of Tibial Bone Density

The bone mineral density (BMD) was monitored and recorded with Lunar-iDXA dual X-ray absorptiometry (GE, Fairfield, CT, USA) at week 0, 1, 2, 4, 6, 8 post-surgery in control and tibia fracture rat model.

Measurement of Trabecular Thickness

The rat tibia was scanned by micro-CT within 2 mm of fracture ends. Each site was serially scanned for 180 consecutive layers with the depth of 14 μm at a voltage of 55 KV and a

current of 145 Ma. Reconstruction was performed with μCT80 Evaluation Program (v6.5-1, Scanco Medical, Bassersdorf, Zurich, Switzerland) and trabecular thickness was calculated (Tb.Th).

Enzyme-Linked Immunosorbent Assay (ELISA)

Serum was isolated from control and surgery model rats. The concentration of inflammatory factors TNF-α, IL-6, IL-4 and bone metabolites alkaline phosphatase (ALP), β cross-linked C-telopeptide of type 1 collagen (β-CTX), procollagen type 1 N-terminal propeptide (P1NP) were measured by ELISA kit following the manufacturer's instruction (Invitrogen, Carlsbad, CA, USA).

HE Staining

Tibia callus tissues were collected at different time points (week 0, 1, 2, 4, 6, 8) and 4% paraformaldehyde was fixed for 24 h. After 5 weeks of decalcification in ethylenediaminetetraacetic acid (EDTA) solution, samples were paraffin-embedded and sliced into 5 μm thin sections. Slides were deparaffinized in xylene for 10 min by 3 times, and rehydrated by serial soaking in anhydrous ethanol 10 min, 95%, 85%, 75% ethanol, respectively, for 5 min. After hematoxylin staining for 10 min, the slides were washed thoroughly with distilled water for 20 min. They were subjected to eosin staining for another 3 min, soaking in 95% anhydrous ethanol for 5 min twice, and in xylene solution for 10 min. Then, slides were mounted in neutral resin for microscope examination.

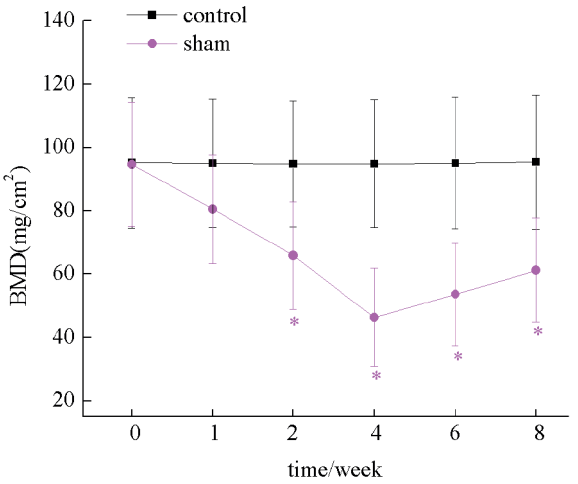

Figure 1. Bone density at different time points of tibia fracture. Bone mineral density (BMD) was determined by Lunar-iDXA dual X-ray absorptiometry and expressed as mineral concentration (mg/cm^2). Each value was representative of at least three individual measurements. *p<0.05 surgery *vs.* control.

Statistical Analysis

Data from three independent experiments were subjected to variance analysis using SPSS19.0 software (SPSS Inc., Armonk, NY, USA), and all the results were presented as mean ± standard deviation (SD). One-way ANOVA method was employed for multiple group comparison analysis and LSD for in-group analysis. The statistical significances between data sets were expressed as p values, and p<0.05 was considered statistically different.

Results

The Change of Bone Density After Tibia Fracture

The bone density was monitored by Lunar-iDXA dual X-ray absorptiometry and the change was showed in Figure 1. We inspected bone density up to 8 weeks after tibia fraction. The bone density was steady in control group, while declined by 30.59% at week 2 and 51.21% at week 4 in sham group rats. From week 6, bone density in the surgical group increased progressively, but still significantly lower than control (p<0.05). Our results showed a two-phase change of bone density during convalescence.

Trabecular Thickness Change in Recovery Phase

Trabecular thickness was evaluated by reconstruction method from μCT data[18] (Figure 2). There was no significant change in our 8-week monitoring period in control groups, which indicated no new bone generation. By contrast, the trabecular thickness in surgical group rats increased dramatically over time, and there was no significant difference between surgical and sham groups at week 8 (p<0.05).

Change of Inflammatory Factors and Bone Metabolic Marker in Serum

Tibia fracture elicited a severe immune reaction and tremendous metabolism shift. We collected serum samples from both control and surgical rats. Serous contents of indicated factors were determi-

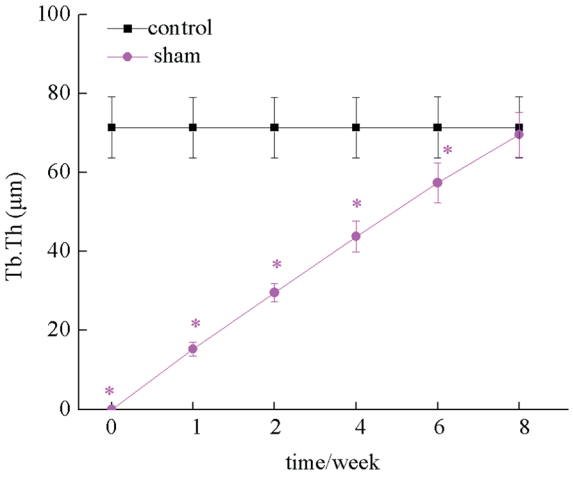

Figure 2. Trabecular thickness change in recovery phase. Trabecular thickness was measured at week 0, 1, 2, 4, 6, 8. Each point represented three independent measurements. *p<0.05 surgical *vs.* Control.

ned by ELISA. Inflammation marker fluctuations were presented in Figure 3. During week 1-2, the concentration of TNF-α and IL-6 in surgical group elevated substantially by 42.14%, 35.42%, 34.50%, 48.18%, respectively, in comparison to the control (p<0.05), which demonstrated marked inflammation progression. The concentration of TNF-α and IL-6 in the surgical group had no significant difference respect the sham group at week 8. However, the concentration of IL-4 in the surgical group was lower (17.25% reduction at week 1 and 34.11% reduction at week 2) than the sham group, and there was no significant difference between surgical and sham groups (p<0.05).

Change of Serous Bone Metabolic Markers in Fracture Rats

ALP is a well-recognized indicator for a bone generation; P1NP and β-CTX for bone resorption. Also, P1NP and β-CTX are highly sensitive biomarkers for bone transformation, and high P1NP corresponded to high transformation rate. As shown in Figure 4, ALP content declined in the sham group from week 1 to 6 and elevated at week 8, while it was still significantly lower than control (p<0.05). By contrast, both P1NP and β-CTX increased at first and reached a maximum of 315.2 ± 29.6 pg/ml, 66.02 ± 7.01 pg/ml respectively in the sham group, while 182.5 ± 19.1 pg/ml, 21.52 ± 3.11 pg/ml in control (p<0.05). These results indicated active bone transformation and generation at week 6.

Upregulation of RUNX2, TGF-β1, VEGF-α, BMP-2, BMP-4, and BMP-7

This RUNX2 is an important transcriptional factor in the osteoblastic differentiation and skeletal morphogenesis. Both TGF-β1 and VEGF-α are potent stimulators of osteoblastic bone formation. BMP-2, BMP-4, and BMP-7 are secreted ligands of TGF-β superfamily, which are involved in osteogenesis[19]. The relative expression of these factors in callus tissue was determined by RT-PCR. As shown in Figure 5, all the indicated factors were upregulated significantly (p<0.05) and peaked at week 6. Moreover, the increases were consistent with bone metabolic index, which further illustrated active osteogenesis at the time point.

Histopathological Change During Coalescence

Next, we attempted to analyze the pathological progression after the operation. Cryo-sections were prepared with callus tissue from both control and sham rats, which were subjected to HE staining following standard protocol and carefully examined by experienced pathologists (Figure 6). Tissue necrosis, periosteal reactive hyperplasia, inflammatory cell infiltration and cell massed, were observed at week 2. The osteoblast was generated at week 4 and fibrous callus connection was developed at week 8 along with chondrogenesis.

Discussion

Tibia is an important bone bearing most of our body weight, which is commonly subjected to fracture caused by automobile collisions, sport injuries or falls from a height[20,21]. Beyond that, tibia fracture also frequently occurs in elderly people who suffer calcium loss and osteoporosis[22], although many could be managed by simple immobilization and rest. The improper treatment of tibia fracture will pose a high risk of disability and bone non-union, which warns of close post-surgical inspection[23].

With the advance of surgical technology, there are currently varieties of choice for operation procedure, which radically rely on the specific medical conditions. In this study, we specifically focused on intramedullary Kirschner wire fixation method in our rat model as it's well established and clinically practiced[24]. Inflammation is the essential event in bone healing[25]. After disruption of vascular structure and extracellular matrix, inflammation was triggered

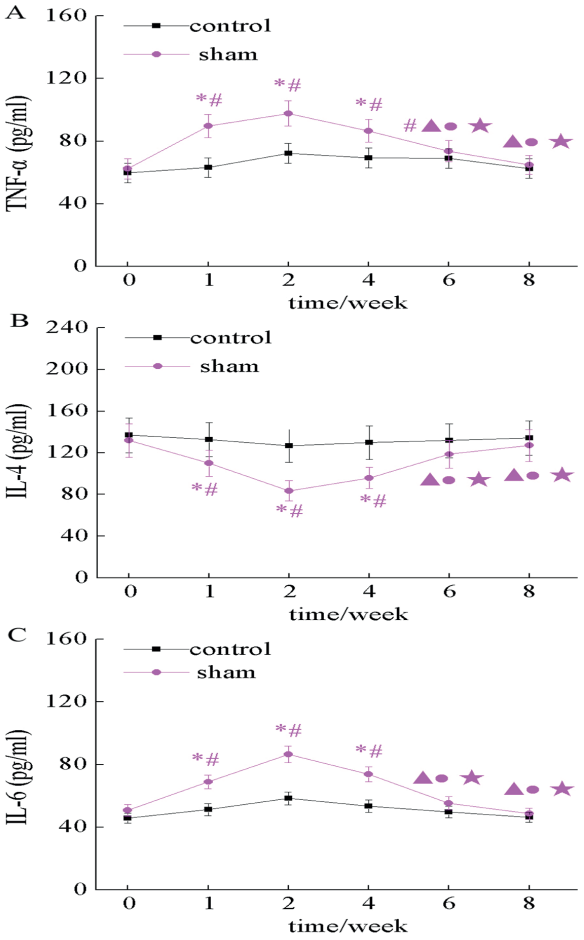

Figure 3. Change of serous inflammatory factors in fracture rats. The indicated factors were measured at week 0, 1, 2, 4, 6, 8. Each data was representative of at least three individual experiments. A: TNF-α; B: IL-4; C: IL-6; #p<0.05 (week 1); ▲p<0.05 (week 2); •p<0.05 (week 4); ★p<0.05 (week 6); ▪p<0.05 (week 8).

by the local generation of stimuli. Inflammatory cells played crucial roles in resorption and regeneration of bone healing, which manifest itself in the form of delayed healing. However, as in many other diseases, inflammation could be a double-edged sword for tibia fracture[26]. The unleashed and over-reactive inflammation may result into non-union, permanent tissue alteration, and chronic disability[27]. The appropriate timing for initiation and termination of acute inflammation is crucial to the healing process. In consistent with this concept[3], our study in the tibia fracture rat model demonstrated that pro-inflammatory factors TNF-α and IL-6 sharply elevated immediately after fracture occurrence. This acute phase of inflammation persisted two weeks in our animal model and was accompanied by a reduction of bone regeneration and an increase of bone resorption. Subsequently, inflammation was progressively suppressed and reversely correlated to increase of proliferation and differentiation. The Runx2 is obligatory for osteoblast differentiation[28], along with other members of TGF-β family, participate in the induction of osteoblast proliferation and differentiation. Expression of these factors was upregulated upon surgery and increased over time during healing, especially at the second half stage, indicating active roles in granulation tissue and callus formation.

Morphological examination of our results also validated the secondary fracture healing process[29]. Bone density declined dramatically in the first 4 weeks, which corresponded to resorption

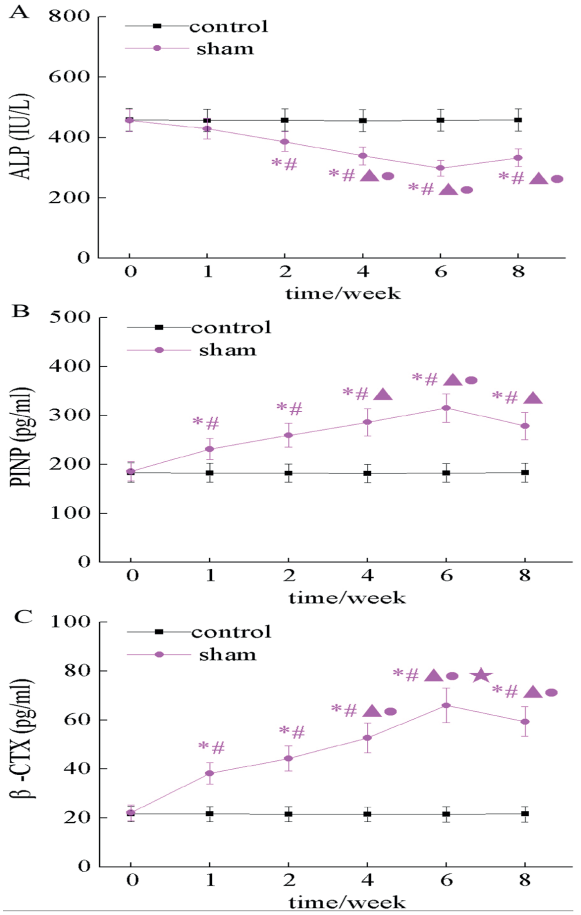

Figure 4. Change of serous bone metabolic marker in fracture rats. The indicated factors were measured at week 0, 1, 2, 4, 6, 8. Each data was representative of at least three individual experiments. A: ALP; B: P1NP; C: β-CTX. #p<0.05 (week 1); ▲p<0.05 (week 2); •p<0.05 (week 4); ★p<0.05 (week 6); ▪p<0.05 (week 8).

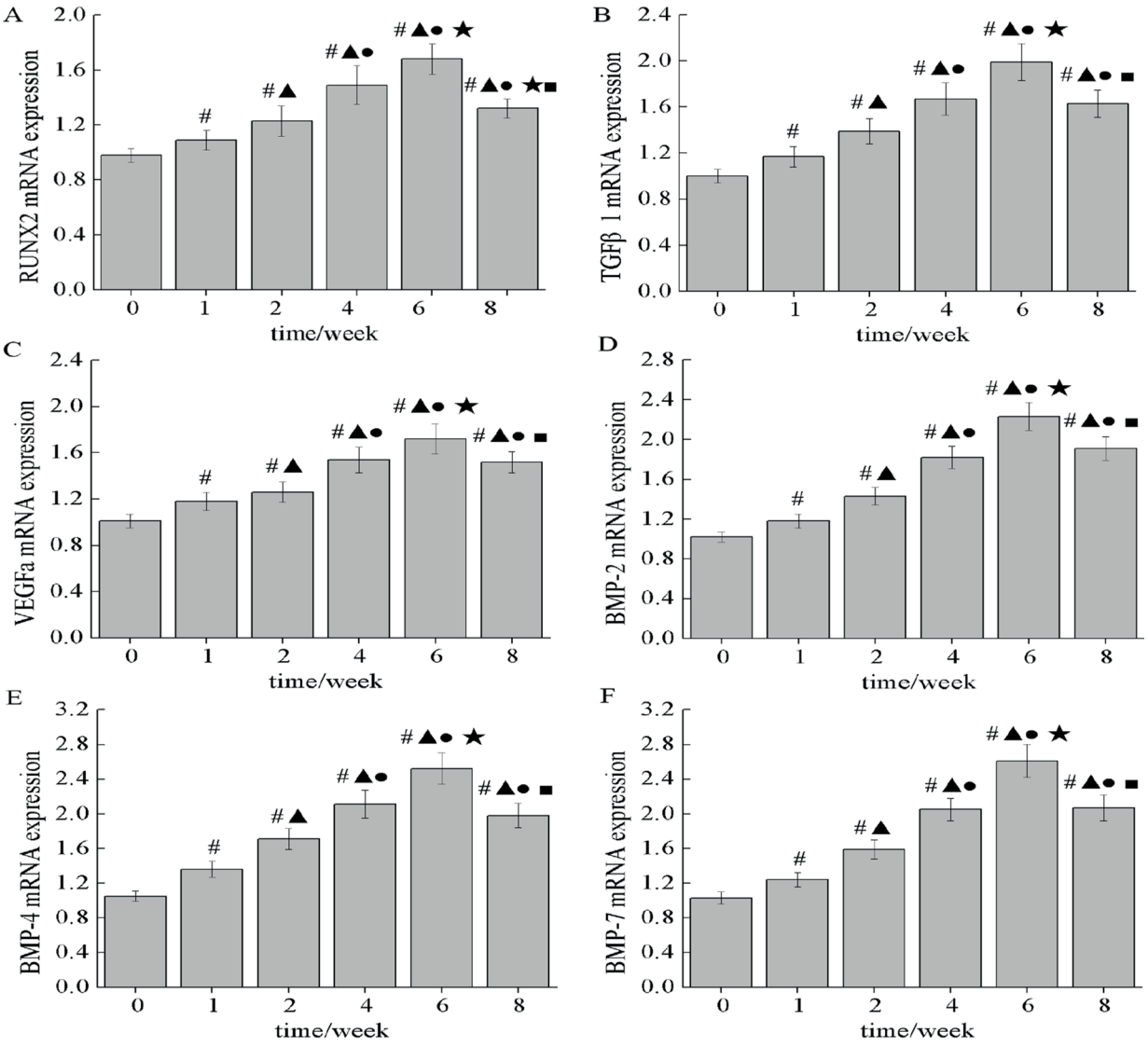

Figure 5. Upregulation of osteogenic factors after fracture. Quantitative Real-time PCR analysis of RUNX2, TGF-β1, VEGF-α, BMP-2, BMP-4 and BMP-7 in callus tissue from sham group. The relative expression was calculated by $2^{-\Delta\Delta Ct}$ method and normalized to GAPDH. Data was presented as Mean ± SD from at least three independent experiments. $^{\#}p<0.05$ (week 1); $^{\blacktriangle}p<0.05$ (week 2); $^{\bullet}p<0.05$ (week 4); $^{\star}p<0.05$ (week 6); $^{\blacksquare}p<0.05$ (week 8).

phase, and then increased with regeneration and remodeling[30]. However, *trabeculae* thickened continuously at fracture sites. Pathological examination of fracture sites further confirmed this process.

Conclusions

We have established and carefully characterized a tibia fracture model in rat for future study. Our model manifested a classical secondary fracture-healing mode, which was validated at molecular, morphological, and pathological level. Given the urgent need for understanding the etiology and biology underlying fracture healing, our study thus contributes to the arsenal for further investigation.

Conflict of Interest

The Authors declare that they have no conflict of interest.

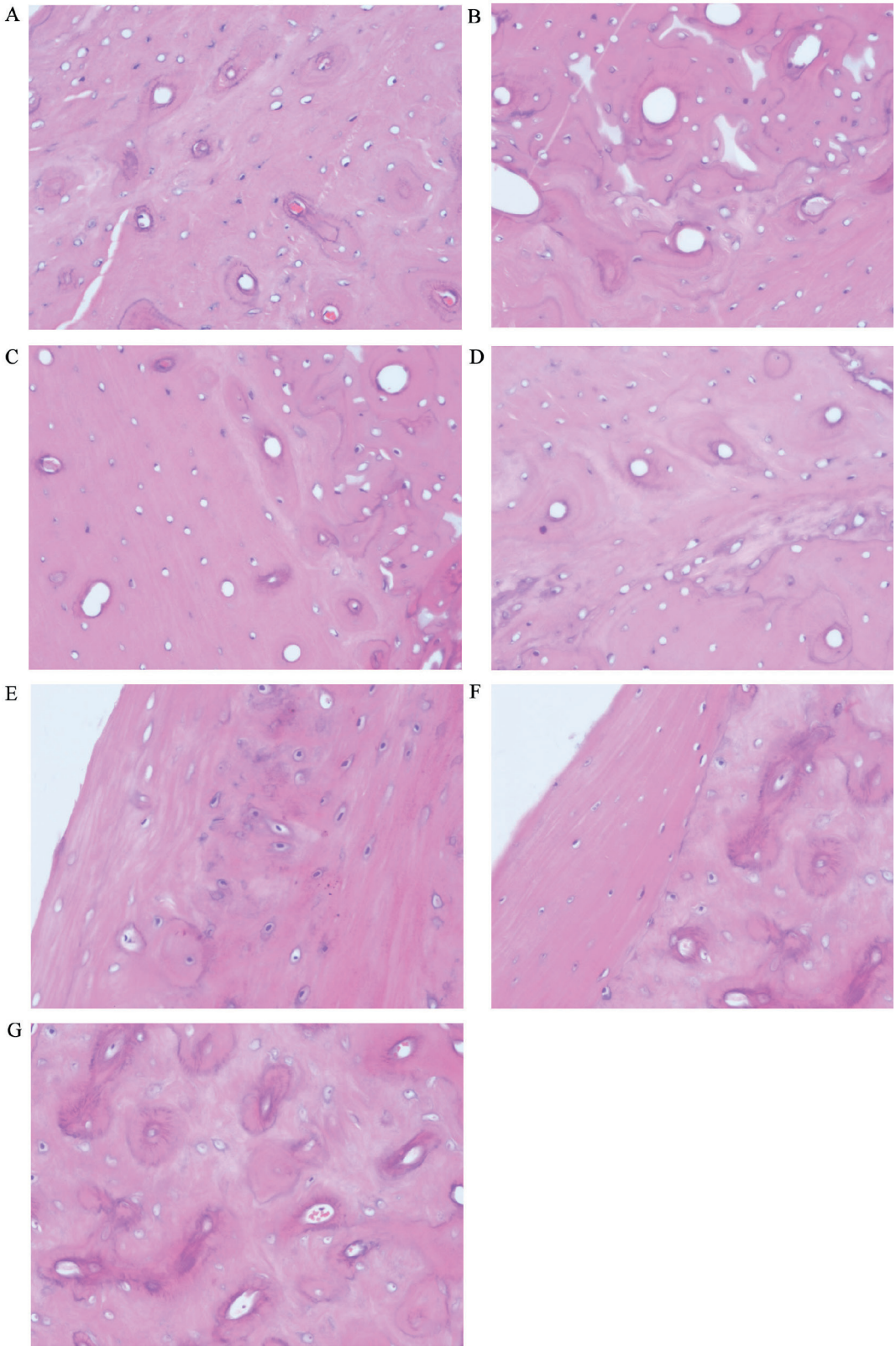

Figure 6. Histopathological alteration in tibia callus tissue (HE ×100).

References

1) Lin X, Xiong D, Peng YQ, Sheng ZF, Wu XY, Wu XP, Wu F, Yuan LQ, Liao EY. Epidemiology and management of osteoporosis in the People's Republic of China: current perspectives. Clin Interv Aging 2015; 10: 1017-1033.
2) De Long WG Jr, Einhorn TA, Koval K, McKee M, Smith W, Sanders R, Watson T. Bone grafts and bone graft substitutes in orthopaedic trauma surgery. A critical analysis. J Bone Joint Surg Am 2007; 89: 649-658.
3) Loi F, Córdova LA, Pajarinen J, Lin TH, Yao Z, Goodman SB. Inflammation, fracture and bone repair. Bone 2016; 86: 119-130.
4) Nakashima T. Regulation of bone homeostasis by bone cells. Clin Calcium 2013; 23: 218-228.
5) Mountziaris PM, Spicer PP, Kasper FK, Mikos AG. Harnessing and modulating inflammation in strategies for bone regeneration. Tissue Eng Part B Rev 2011; 17: 393-402.
6) Lapérine O, Blin-Wakkach C, Guicheux J, Beck-Cormier S, Lesclous P. Dendritic-cell-derived osteoclasts: a new game changer in bone-resorption-associated diseases. Drug Discov Today 2016; 21: 1345-1354.
7) Mantovani A, Biswas SK, Galdiero MR, Sica A, Locati M. Macrophage plasticity and polarization in tissue repair and remodelling. J Pathol 2013; 229: 176-185.
8) Marsell R, Einhorn TA. The biology of fracture healing. Injury 2011; 42: 551-555.
9) Kolar P, Schmidt-Bleek K, Schell H, Gaber T, Toben D, Schmidmaier G, Perka C, Buttgereit F, Duda GN. The early fracture hematoma and its potential role in fracture healing. Tissue Eng Part B Rev 2010; 16: 427-434.
10) Claes L, Recknagel S, Ignatius A. Fracture healing under healthy and inflammatory conditions. Nat Rev Rheumatol 2012; 8: 133-143.
11) Wu AC, Raggatt LJ, Alexander KA, Pettit AR. Unraveling macrophage contributions to bone repair. Bonekey Rep 2013; 2: 373.
12) Schindeler A, McDonald MM, Bokko P, Little DG. Bone remodeling during fracture repair: the cellular picture. Semin Cell Dev Bio 2008; 19: 459-466.
13) Keramaris NC, Calori GM, Nikolaou VS, Schemitsch EH, Giannoudis PV. Fracture vascularity and bone healing: a systematic review of the role of VEGF. Injury 2008; 39 Suppl 2: S45-57.
14) Malizos KN, Papatheodorou LK. The healing potential of the periosteum molecular aspects. Injury 2005; 36 Suppl 3: S13-S19.
15) Tsiridis E, Upadhyay N, Giannoudis P. Molecular aspects of fracture healing: which are the important molecules? Injury 2007; 38 Suppl 1: S11-S25.
16) McKibbin, B. The biology of fracture healing in long bones. J Bone Joint Surg Br 1978; 60-B: 150-162.
17) Reikeras O, Winge MI, Rokkum M. Effect of soft-tissue attachment on tibial fracture healing in rats. J Orthop Surg (Hong Kong) 2015; 23: 47-51.
18) Vieira AE, Repeke CE, Ferreira Junior Sde B, Colavite PM, Biguetti CC, Oliveira RC, Assis GF, Taga R, Trombone AP, Garlet GP. Intramembranous bone healing process subsequent to tooth extraction in mice: micro-computed tomography, histomorphometric and molecular characterization. PLoS One 2015; 10: e0128021.
19) Imai Y, Terai H, Nomura-Furuwatari C, Mizuno S, Matsumoto K, Nakamura T, Takaoka K. Hepatocyte growth factor contributes to fracture repair by upregulating the expression of BMP receptors. J Bone Miner Res 2005; 20: 1723-1730.
20) Matcuk GR Jr, Mahanty SR, Skalski MR, Patel DB, White EA, Gottsegen CJ. Stress fractures: pathophysiology, clinical presentation, imaging features, and treatment options. Emerg Radiol 2016; 23: 365-375.
21) Angthong C, Krajubngern P, Tiyapongpattana W, Pongcharoen B, Pinsornsak P, Tammachote N, Kittisupaluck W. Effects of renal function on the intraosseous concentration and inhibitory effect of prophylacticcefazolin in knee arthroplasty. Eur Rev Med Pharmacol Sci 2016; 20: 5216-5222.
22) Torres-del-Pliego E, Vilaplana L, Güerri-Fernández R, Diez-Pérez A. Measuring bone quality. Curr Rheumatol Rep 2013; 15: 373.
23) Gómez-Barrena E, Rosset P, Lozano D, Stanovici J, Ermthaller C, Gerbhard F. Bone fracture healing: cell therapy in delayed unions and nonunions. Bone 2015; 70: 93-101.
24) Marvan J, Džupa V, Bartoška R, Kachlík D, Krbec M, Báča V. Kirschner wire transfixation of unstable ankle fractures: indication, surgical technique and outcomes. Acta Chir Orthop Traumatol Cech 2015; 82: 216-221.
25) Serhan CN, Savill J. Resolution of inflammation: the beginning programs the end. Nat Immunol 2005; 6: 1191-1197.
26) Tavares LP, Teixeira MM, Garcia CC. The inflammatory response triggered by Influenza virus: a two edged sword. Inflamm Res 2017; 66: 283-302.
27) Copuroglu C, Calori GM, Giannoudis PV. Fracture non-union: who is at risk? Injury 2013; 44: 1379-1382.
28) Stein GS, Lian JB, van Wijnen AJ, Stein JL, Montecino M, Javed A, Zaidi SK, Young DW, Choi JY, Pockwinse SM. Runx2 control of organization, assembly and activity of the regulatory machinery for skeletal gene expression. Oncogene 2004; 23: 4315-4329.
29) Hildebrand T, Laib A, Müller R, Dequeker J, Rüeggsegger P. Direct three-dimensional morphometric analysis of human cancellous bone: microstructural data from spine, femur, iliac crest, and calcaneus. J Bone Miner Res 1999; 14: 1167-1174.
30) Gunczler P, Lanes R, Paoli M, Martinis R, Villaroel O, Weisinger JR. Decreased bone mineral density and bone l Metab 2001; 14: 525-528.